

On the Evaluation and Refinement of Vision-Language Instruction Tuning Datasets

Ning Liao¹, Shaofeng Zhang¹, Renqiu Xia¹, Min Cao³, Yu Qiao², Junchi Yan^{1*}

¹Shanghai Jiao Tong University, Shanghai, 200240, China.

²Shanghai Artificial Intelligence Laboratory, Shanghai, 200030, China.

³Soochow University, Suzhou, 215006, China.

*Corresponding author(s). E-mail(s): yanjunchi@sjtu.edu.cn;

Contributing authors: liaoning@sjtu.edu.cn; sherrylone@sjtu.edu.cn; xiarenqiu@sjtu.edu.cn; caomin0719@126.com; qiaoyu@pjlab.org.cn;

Abstract

There is an emerging line of research on multimodal instruction tuning, and a line of benchmarks has been proposed for evaluating these models recently. Instead of evaluating the models directly, in this paper, we try to evaluate the Vision-Language Instruction-Tuning (VLIT) datasets. Also, we seek the way of building a dataset for developing an all-powerful VLIT model, which we believe could also be of utility for establishing a grounded protocol for benchmarking VLIT models. For effective evaluation of VLIT datasets that remains an open question, we propose a *tune-cross-evaluation* paradigm: tuning on one dataset and evaluating on the others in turn. For each single tune-evaluation experiment set, we define the Meta Quality (MQ) as the mean score obtained by a set of caption metrics including BLEU, METEOR, and ROUGE-L to quantify the quality of a certain dataset or a sample. On this basis, to evaluate the comprehensiveness of a dataset, we develop the Dataset Quality (DQ) covering all tune-evaluation sets. To lay the foundation for building a comprehensive dataset and developing an all-powerful model for practical applications, we define the Sample Quality (SQ) to quantify the all-sided quality of each sample. Extensive experiments validate the rationality of the proposed evaluation paradigm. Based on the holistic evaluation, we build a new dataset, REVO-LION (REfining VisiOn-Language InstructiOn tuNing), by collecting samples with higher SQ from each dataset. Remarkably, even with only half of the complete data, the model trained on REVO-LION can achieve the performance comparable to simply adding all VLIT datasets up. Furthermore, REVO-LION not only facilitates the development of a powerful model but also incorporates an evaluation set, which is designed to serve as a convenient benchmark for future research in the field.

Keywords: Vision-language, instruction tuning, evaluation, refinement.

1 Introduction

The large-scale multimodal model GPT-4 (OpenAI, 2023) has recently exhibited strong power in generating desired answers from given images and instructions. Inspired by its remarkable success, various multimodal instruction tuning models (Dai et al., 2023; Chen et al., 2023; Li et al., 2023; Luo et al.,

2023) have been proposed towards different aspects of Vision-Language (VL) understanding, such as MiniGPT-4 (Zhu et al., 2023) for detailed description and LLaVAR (Zhang et al., 2023) for text-rich image understanding. With the rapid development of Vision-Language Instruction-Tuning (VLIT), evaluating these models becomes increasingly important, for

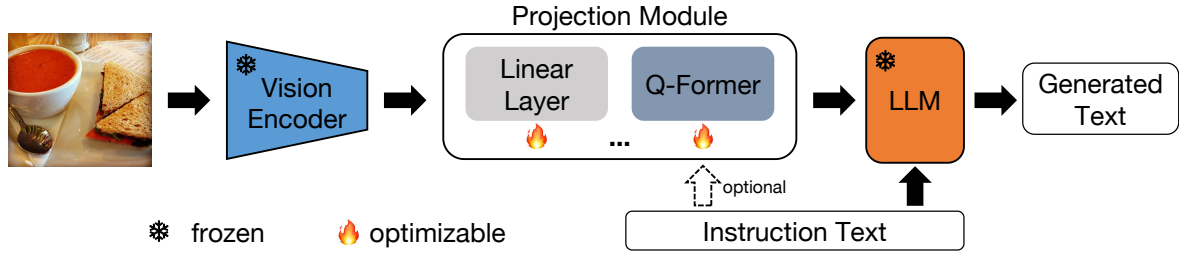


Fig. 1 The popular architecture in current vision-language instruction tuning methods (Dai et al., 2023; Liu et al., 2023). Extracting the visual feature by a frozen image encoder, transferring the visual feature into the language space using an optimizable projection module, and generating text output via a frozen Large Language Model (LLM).

which several benchmarks (Yin et al., 2023; Xu et al., 2023; Liu et al., 2023) are very recently released.

Different from these existing benchmarks that concentrate on evaluating VLIT models directly, our goal is one step back: **evaluating VLIT datasets**. The motivation comes from the insights into current VLIT models, including two similarities and one difference. *The first similarity is the model architecture* as shown in Fig. 1. The image feature is firstly extracted by a frozen vision encoder (Fang et al., 2023). Then, a learnable projection module, which can be simply designed either as the linear layer in LLaVA (Liu et al., 2023) or a more sophisticated one like Q-Former in InstructBLIP (Dai et al., 2023), transforms the image feature to the text space. Finally, by feeding the transformed image feature and instruction text into the frozen Large Language Models (LLMs) (Touvron et al., 2023; Chiang et al., 2023), the instruction-following answer is generated. *The second similarity is the two-stage learning scheme*. During training, common large-scale image-text pairs (Ordonez et al., 2011; Schuhmann et al., 2021; Sharma et al., 2018) are leveraged for the cross-modal feature alignment in the first stage. Then, the customized high-quality instruction data is used to train the VLIT model to generate coherent and desired output in the second stage. *The difference is exactly the high-quality instruction data targeting at different aspects of VL understanding*, as concluded in Table 1. To be more consistent with LLMs, the annotations in these datasets are almost generated or augmented by GPT. It follows that curating proper instruction tuning datasets is essential in VLIT, which motivates us to evaluate VLIT datasets and look into their quality.

However, there exist limitations when using current benchmarks for evaluation. For example, in benchmarks (Xu et al., 2023; Liu et al., 2023), the style

of annotations is quite different from the style of the open-ended texts generated by LLMs, causing possible bias for assessment. Besides, human voting (Xu et al., 2023) and ChatGPT/GPT-4 (OpenAI, 2023) are leveraged for performance evaluation. While the former is labor-intensive and liable to cause subjective evaluation, and the latter is inconvenient and unstable for widespread use because of the API availability and the changeable output. Additionally, it is worth noting that although evaluations utilizing GPT models have demonstrated the highest agreement with human evaluations (Bitton et al., 2023), both GPT models and human evaluation are not well-suited for large-scale evaluation scenarios due to practical considerations.

To conduct a comprehensive analysis of VLIT datasets, we introduce a pioneering *tune-cross-evaluation* paradigm, as shown in Fig. 2, based on the common architecture in Fig. 1. This paradigm allows us to thoroughly assess the datasets. The fundamental concept is that each dataset serves a dual purpose: it can be utilized for model development and also function as a benchmark for the specific aspect it was designed to address. Our evaluation paradigm benefits from annotations consistent with LLMs, enabling us to define the Meta Quality (MQ) as the average score measured by caption metrics, including BLEU, METEOR, and ROUGE-L. This model-free and human-free evaluation strategy, utilizing MQ to measure performance in each tune-evaluation experiment set, offers greater convenience and stability than GPT-involved scoring and a more objective assessment than human voting. Building upon the proposed MQ, we devise the concepts of Dataset Quality (DQ) and Sample Quality (SQ) to measure the overall capability of each dataset and sample, combining all tune-evaluation sets.

Taking a step further, the other goal in this paper is **refining VLIT datasets** according to the holistic evaluation on a set of VLIT datasets. On one hand, existing VLIT models are only equipped with one or several abilities in VL understanding, which leads to unsatisfying performance in comprehensive evaluations. On the other hand, existing benchmarks build evaluation datasets by collecting datasets from different tasks (Krizhevsky et al., 2009; Lu et al., 2022) with annotations inconsistent with the open-ended generated texts (Xu et al., 2023; Yin et al., 2023), which causes inaccurate evaluation. As a result, a dataset encompassing multiple VLIT capabilities is critical for developing an all-powerful model and building an unbiased benchmark in a convenient way.

To this end, we build the so-called REVO-LION dataset by REfining ViSiOn-Language InstructiOn tuNing datasets, which is composed of samples with higher SQ from each dataset as listed in Table 1. As a compact subset of the original datasets, REVO-LION is shown empirically to be more sample-efficient than simply merging the raw datasets together, which validates the effectiveness of the proposed SQ and the refinement strategy. We make following contributions:

- We propose a *tune-cross-evaluation* paradigm on VLIT datasets. To our best knowledge, this is the first holistic analysis on VLIT datasets.
- We define a model-free and human-free evaluation metric known as the Meta Quality (MQ), as the mean score measured by BLEU, METEOR, and ROUGE-L. Based on MQ, Dataset Quality (DQ) and Sample Quality (SQ) are devised to quantify the comprehensive quality of each dataset and sample in VLIT, respectively.
- We collect and release a comprehensive dataset called REVO-LION, by refining public mainstream VLIT datasets. REVO-LION consists of a training set for developing a highly capable VLIT model and an evaluation set that serves as an effective benchmark. Extensive experiments show that in addition to expanding the data scale, collecting high-quality data based on rational and effective evaluation is crucial for the advancement of VLIT models.

2 Related Work

2.1 Vision-Language Instruction Tuning

With the success of ChatGPT and InstructGPT (Ouyang et al., 2022) in solving tasks aligned

with human instructions, subsequent Large Language Models (LLMs) (Peng et al., 2023; Ding et al., 2023; Zhou et al., 2023; Du et al., 2022) have been further devised by fine-tuning open-source LLMs such as LLaMA (Touvron et al., 2023) and GLM (Zeng et al., 2022) using instruction data in the last two years. For example, Vicuna-13B (Chiang et al., 2023) is supervised fine-tuned from LLaMA-13B (Touvron et al., 2023) using 70K shared conversations with ChatGPT from ShareGPT.com; Alpaca-7B (Taori et al., 2023) is fine-tuned from LLaMA-7B (Touvron et al., 2023) on 52K instruction-following demonstrations generated by Self-Instruct (Wang et al., 2022).

Standing on the shoulder of LLMs, many Vision-Language Instruction Tuning (VLIT) models (Su et al., 2023; Ye et al., 2023; Luo et al., 2023; Li et al., 2023; Aiello et al., 2023) have been proposed within a year. These models are similarly constructed by using a projection module to connect the pre-trained vision model for visual perception and the language model for text generation. The projection module is firstly trained on common image-text pairs for VL alignment, then on high-quality data for instruction tuning. One of the most impactful methods is InstructBLIP (Dai et al., 2023), which is built upon the VL alignment achieved by the Q-Former in BLIP2 (Li et al., 2023). After collecting and transforming 28 datasets from 11 tasks into instruction format, InstructBLIP (Dai et al., 2023) takes the instruction as a guidance of Q-Former to extract instruction-aware visual features for further tuning. Similar to InstructBLIP, MiniGPT-4 (Zhu et al., 2023) is firstly pre-trained on large-scale datasets (Ordonez et al., 2011; Schuhmann et al., 2021) for VL alignment, then curates around 3500 high-quality instruction data, with the assistance of ChatGPT and Vicuna (Chiang et al., 2023) targeting at comprehensive image description, for instruction tuning in the second stage. LRV (Liu et al., 2023) constructs a dataset including both positive and negative instructions for robust tuning with mitigated hallucination issues based on MiniGPT-4. Simpler than MiniGPT-4, LLaVA (Liu et al., 2023) adopts a linear layer to bridge the gap between visual and language space in the first stage using 595K image-text pairs filtered from CC3M. Then, by using ChatGPT and GPT-4, 158K instruction samples including conversations, detailed descriptions, and complex reasoning are collected in LLaVA for instruction tuning in the second stage. Similar to LLaVA (Liu et al., 2023), DetGPT (Pi et al., 2023) collects around 30K query-answer pairs

Table 1 Popular vision-language instruction tuning datasets on current VLIT methods. These datasets are used to build the proposed REVO-LION in this paper.

Datasets	Size	Purpose
DetGPT (Pi et al., 2023)	50K images and around 30K query-answer pairs	Reasoning-based object detection.
LAMM (Yin et al., 2023)	186K image-language instruction-response pairs	Daily conversation, factual knowledge reasoning, detailed description, visual task dialogue.
LLaVAR (Zhang et al., 2023)	16K high-quality instruction following data.	Text-rich image understanding
LLaVA (Liu et al., 2023)	58K in conversations, 23K in detailed description, 77K in complex reasoning.	Conversations, detailed description, complex reasoning.
Macaw (Lyu et al., 2023)	69K image instances.	Human-written style text generation.
MiniGPT-4 (Zhu et al., 2023)	Around 3.5K image-text pairs.	Comprehensive image description.
LRV (Liu et al., 2023)	Around 120K instances.	Robust visual instruction with mitigated hallucination issue.

towards reasoning-based object detection for instruction tuning in the second stage, LLaVAR (Zhang et al., 2023) enhances the text-rich image understanding ability by collecting 16K text-rich image data, Macaw (Lyu et al., 2023) builds a dataset consisting of 69K instances for human-style text generation.

To make a brief summary, existing VLIT models mostly share the similar model architecture and the two-stage learning scheme. The major difference lies in the high-quality instruction data used in the second stage. Beyond current VLIT models targeting at certain aspects, as concluded in Table 1, collecting a comprehensive dataset lies the foundation for developing an all-powerful VLIT model.

2.2 VLIT Benchmarks

With the rapid development of VLIT models, how to comprehensively and effectively evaluate these models becomes a concurrent significant problem. To this end, several benchmarks (Zeng et al., 2023; Yu et al., 2023; Bitton et al., 2023) have been proposed in the last few months. The pioneering benchmark is the LVLM-eHub (Xu et al., 2023), which evaluates VLIT models by quantifying the performance and human voting in the online arena platform. In performance quantification, they utilize 47 standard benchmarks covering 6 capabilities for evaluation, and find that image caption metrics are ineffective because the style of open-ended generated texts differs from that of annotations in the benchmarks. It

is reasonable because the annotations in these benchmarks are rough, simple and outdated in the context of LLMs. Immediately after LVLM-eHub, LAMM (Yin et al., 2023) is proposed for evaluation on 9 common image tasks by collecting 11 datasets. Except for task-specific metrics, LAMM adopts GPT as a judgment for performance evaluation. However, MME (Fu et al., 2023) argues that human voting and GPT scoring bring problems of subjectivity and inaccuracy. For this, MME exams perception and cognition abilities covering 14 subtasks by manually constructing instruction-answer pairs and leading the tested models to answer “yes” or “no”, which is designed for objective and accurate quantitative statistics. Nevertheless, such performance evaluation that heavily relies on generating “yes” or “no” is not quite reasonable, because existing VLIT models usually target at detailed tasks instead of making decisions from “yes” or “no” strictly. For fine-grained ability assessment, MMBench (Liu et al., 2023) curates a dataset covering 20 fine-grained skills, and all instances are transformed into multi-choice problems. For robust evaluation, it employs ChatGPT for answer extraction and judgment in the proposed circular evaluation strategy, which is unable to evaluate the models directly on the generated texts, causing inaccurate assessment.

In short, there are three aspects that are not fully satisfied in existing benchmarks: 1) collecting datasets with annotations consistent with open-ended generated texts for evaluation; 2) avoiding human subjectivity in data selection and evaluation; 3) designing stable

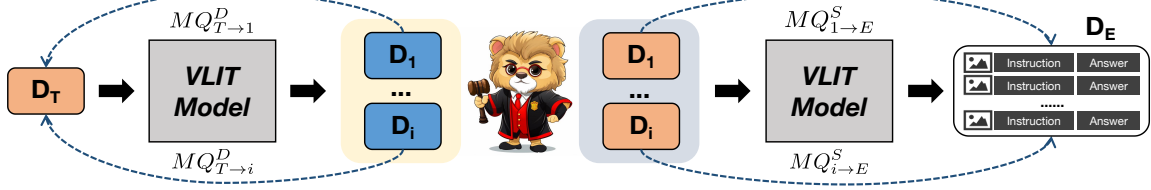


Fig. 2 The overall framework of the proposed *tune-cross-evaluation* paradigm. *Left*: The diagram of Dataset Quality (DQ) evaluation. Each dataset adopted for testing measures the quality of the tuning dataset D_T on the aspect that the testing datasets are constructed towards. *Right*: The diagram of Sample Quality (SQ) evaluation. Each dataset used for tuning measures how well the samples in the testing set D_E match with the ability that the tuning dataset is constructed towards.

and convenient quantification metrics. We argue that it is possible to meet these conditions via our *tune-cross-evaluation* paradigm on VLIT datasets with the proposed quality metrics at both dataset and sample levels. In particular, based on our deep dive in Sec. 2.1, we propose shifting the focus of model evaluation, which existing benchmarks are paying great efforts on, to dataset evaluation.

3 Methodology

3.1 Tune-Cross-Evaluation Paradigm

As shown in Fig. 2, we propose the *tune-cross-evaluation* paradigm to evaluate VLIT datasets, which are specifically listed in Table 1. Note that these datasets are all in English such that we do not need to handle the language bias problem, which is also not the focus of this paper. On one hand, each dataset is employed to develop a model by instruction tuning. On the other hand, because these VLIT datasets are almost annotated by leveraging GPT-4 (OpenAI, 2023) or ChatGPT for text generation or augmentation, each dataset also represents a standard on the aspect that the dataset is constructed towards, by which the proper annotations consistent with open-ended generated texts are accessible. Based on the VL alignment learned in the first stage by the model with the architecture in Fig. 1, at each time, we select one dataset from these datasets for instruction tuning, and the remaining datasets are used for test at this time. For example, when we use DetGPT (Pi et al., 2023) for instruction tuning, the tuned model equipped with great reasoning-based object detection ability will be further tested on other datasets, and they involve testing the model’s ability such as daily conversation, factual knowledge reasoning, detailed description, etc. By taking turns to cycle in this way, we finally get the comprehensive quality evaluation of each dataset and each sample. To quantify the comprehensiveness,

we define the Meta Quality (MQ), Dataset Quality (DQ) and Sample Quality (SQ), and detail them in the following sections.

3.2 Meta Quality (MQ)

In LVLm-eHub (Xu et al., 2023), the authors show that metrics in caption tasks are ineffective for VLIT evaluation due to the style differences between the diverse open-ended generated texts and the ground-truths in the datasets curated prior to LLMs, which are outdated compared to LLMs. Benefiting from the proposed *tune-cross-evaluation* paradigm, when making full use of VLIT datasets as evaluation ones, the proper annotations, which are created by GPT models to be consistent with LLMs, are available. Therefore, with mitigated style differences, to perform a model-free and human-free evaluation, in which we do not rely on other models such as GPT or human for scoring, we define the Meta Quality (MQ) as the average of scores measured by caption metrics to quantify the one-side quality of each dataset or sample within a single tune-evaluation experiment. Considering the time-consuming process in calculating sample-wise MQ if using SPICE, we use BLEU@1 (B@1), BLEU@2 (B@2), BLEU@3 (B@3), BLEU@4 (B@4), METEOR (M), and ROUGE-L (R) as the components for MQ definition. CIDEr is set as a hold-out metric in data refinement in Sec. 4.6. The MQ is formulated as:

$$MQ = \text{mean}(B@1 + B@2 + B@3 + B@4 + M + R). \quad (1)$$

The ablation of the combinations is studied in Sec. 4.4. It should be noted that the MQ can be commonly used to measure on a set of samples. When the number of samples is 1, it actually measures the sample-wise quality. For distinction, we denote the MQ measured on a dataset and a sample as MQ^D and MQ^S , respectively.

3.3 Dataset Quality (DQ)

In the proposed *tune-cross-evaluation* paradigm, each time we select a dataset denoted as D_T from the set of datasets S for instruction tuning, the remaining datasets denoted as $D_i (i \in S, i \neq T)$ are then leveraged as evaluation ones for inference, thus measuring the quality of the tuning dataset on the aspect that the evaluation datasets are constructed towards one by one, as shown on the left side of Fig. 2. Note that though the datasets to be evaluated in this paradigm are in different sizes, we do not explicitly separate a metric for data size. When using a dataset as an evaluation one, its size has been implicitly integrated into the measurement. A dataset with larger size is more likely to exhibit better comprehensive ability, as compared between LLaVA-Detailed description and MiniGPT-4, which both concentrate on detailed image description in Table 4 in experiments. In a single tune-evaluation set, the one-side dataset quality is denoted as $MQ_{T \rightarrow i}^D$, in which the right arrow indicates the direction from the tuning dataset to the evaluation dataset. Specifically, we set the quality $MQ_{T \rightarrow T}^D$ that each tuning dataset exhibits on its aspect as 1, the maximum value of MQ . Therefore, when a dataset is set as the tuning one, its comprehensive quality measured by all capabilities in S is formulated as the sum of all one-side qualities:

$$\begin{aligned} DQ_T &= MQ_{T \rightarrow T}^D + \sum_{i \in S, i \neq T} MQ_{T \rightarrow i}^D \\ &= 1 + \sum_{i \in S, i \neq T} MQ_{T \rightarrow i}^D, T \in S. \end{aligned} \quad (2)$$

By setting each dataset as the tuning one and the remaining as evaluation ones in turn, the comprehensive DQ, which measures various capabilities, for all datasets can be calculated.

3.4 Sample Quality (SQ)

Because the MQ can only be calculated on the inference datasets, it is hard to measure the quality of each sample in the tuning dataset when keeping the same evaluation direction in DQ, i.e., the inference datasets are regarded as standards. In contrast, when a dataset D_E is set as the inference one, we hold that the model equipped with the ability of dataset $D_i (i \in S, i \neq E)$, after tuned on which, is supposed to be a standard. By this way, the $MQ_{i \rightarrow E}^S$ for each sample in D_E measures how close the sample matches with the ability

of the tuning dataset D_i , as shown on the right side of Fig. 2. To calculate the comprehensive quality that each sample exhibits on other aspects, other than DQ having the ability corresponding to itself, we define the SQ as a weighted sum:

$$SQ_E = \sum_{i \in S, i \neq E} DQ_i \cdot MQ_{i \rightarrow E}^S. \quad (3)$$

We use the DQ_i as the weights for objective evaluation, the higher DQ_i represents a more confident evaluation when using dataset D_i to tune the model, which is regarded as a standard. By setting each dataset as the inference one and the remaining as tuning ones in turn, the comprehensive SQ for each sample exhibits on other datasets can be calculated.

3.5 REVO-LION

To build a comprehensive dataset integrating all capabilities of the evaluated datasets, a simple yet direct way is to merge these datasets into one without more operations. As suggested in the analysis (Zeng et al., 2023), data quality is more significant than data quantity. Therefore, we propose to Refine VisiOn-Language InstructiOn tuNing (REVO-LION) datasets according to the proposed SQ, which measures the comprehensive quality of each sample exhibits on other datasets. To preserve all capabilities, we collect samples with higher SQ from each dataset to compose REVO-LION. Formally, we denote the portion that the number of selected samples to the number of all samples in each dataset as P . The lower bound of SQ in dataset $D_i (i \in S)$ corresponding to the portion P is τ_i^P . For each sample $\mathbf{x}_i^k \in D_i$, if the SQ of it SQ_i^k is no lower than τ_i^P , the sample is collected in REVO-LION, which is formulated as:

$$S1 = \bigcup_{i \in S} \mathbf{x}_i^k, \quad (\mathbf{x}_i^k \in D_i, SQ_i^k \geq \tau_i^P). \quad (4)$$

We denote this refinement strategy as $S1$, which is validated to be more effective than ‘‘Random Refinement’’ ($S2$) and ‘‘Gaussian Refinement’’ ($S3$) in Sec. 4.6. After performing the data evaluation and creating REVO-LION from the datasets in Table 1, we split it into a training set and an evaluation set. The former can serve as a common dataset for developing an all-powerful VLIT model, and the latter can serve as a convenient benchmark covering all capabilities

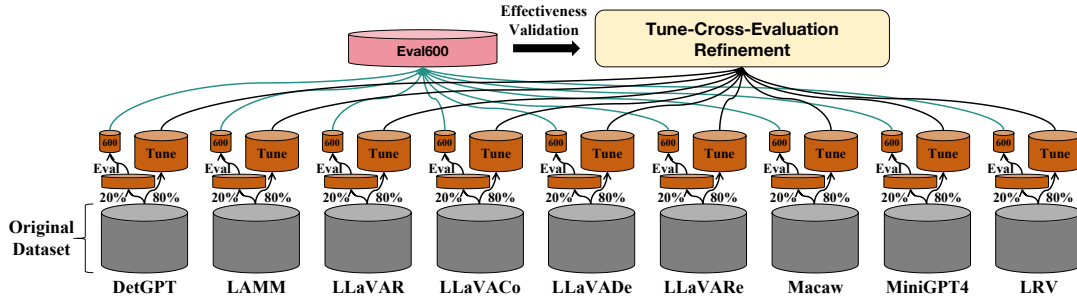


Fig. 3 The diagram of the data split process. It is designed to validate the effectiveness of the proposed *tune-cross-evaluation* paradigm and the data refinement strategy in main experiments. Each original dataset is divided into two parts: 80% samples are collected as a tuning set for data evaluation and refinement, and 600 samples from the remaining 20% are collected into a balanced and comprehensive evaluation set. For robust validation, we perform such partitions twice, thus creating SPLIT1 and SPLIT2 that are used in the main experiments.

of these datasets and equipping with ideal annotations, based on which the caption metrics can be conveniently employed for model-free and human-free evaluation.

4 Experiments

4.1 Implementation Details

Data Preparation. The evaluated VLIT datasets are clarified in Table 1. Specifically, to ensure that each dataset is independent of each other and has no overlapping samples, in DetGPT (Pi et al., 2023), we remove samples generated from MiniGPT-4 (Zhu et al., 2023); in LLaVAR (Zhang et al., 2023), we remove samples generated from LLaVA (Liu et al., 2023). Concentrating on the vision-language field, in LAMM (Yin et al., 2023) and Macaw (Lyu et al., 2023), we only use the released image-text data. In addition, the data in LLaVA (Liu et al., 2023) is divided into three independent ones: LLaVA-Conversation (LLaVACo), LLaVA-Detailed description (LLaVAde) and LLaVA-Reasoning (LLaVARE) for their clear difference.

To validate the effectiveness of the proposed data refinement strategy, we need to design an evaluation set covering all capabilities of these datasets. For this, we collect 80% samples from each dataset to build independent training sets, on which the *tune-cross-evaluation* paradigm and refinement are performed, and collect 600 samples from the remaining 20% samples to build a balanced and comprehensive evaluation set, namely *Eval600*, as shown in Fig. 3. We choose 600 samples from each dataset for testing because the smallest dataset MiniGPT-4 (Zhu et al., 2023) includes about 3,500 samples, and the 20% includes no more

Table 2 The hyperparameters for instruction tuning using the architecture of InstructBLIP (Dai et al., 2023), which adopts the Q-Former as the projection module.

Hyperparameters	
Epochs	5
Warmup Epochs	1
Warmup initial learning rate	1e-8
Warmup end learning rate	1e-5
Warmup Schedule	Linear
Learning rate decay	Cosine
End (Minimum) learning rate	0
Batch size	128
Optimizer	AdamW
AdamW β	(0.9, 0.999)
Weight decay	0.05

Table 3 The hyperparameters for instruction tuning using the architecture of LLaVA (Liu et al., 2023), which adopts the linear layer as the projection module.

Hyperparameters	
Epochs	3
Learning rate	2e-5
Learning rate decay	Cosine
Batch size	128
Optimizer	AdamW
Weight decay	0.0

than 700 samples. To build a balanced and comprehensive evaluation set, we finally set the number of selected samples from each dataset for evaluation as 600. To verify the effectiveness of the proposed evaluation paradigm and data refinement on different data partitions, and ensure the universality of experimental effect verification, we perform such data split twice and get two sets, denoted as SPLIT1 and SPLIT2.

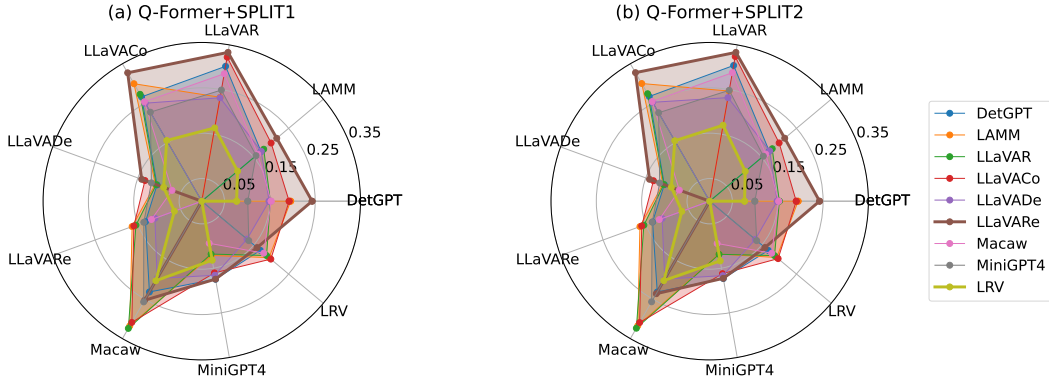


Fig. 4 Visualizations of $MQ_{T \rightarrow i}^D (i \neq T)$ in dataset quality evaluation. Lines with different colors represent different datasets D_T used for instruction tuning.

Table 4 DQ evaluated on SPLIT1 and SPLIT2 by using the Q-Former based architecture.

D_T	DetGPT	LAMM	LLaVAR	LLaVACo	LLaVADe	LLaVARE	Macaw	MiniGPT-4	LRV
Q-Former+SPLIT1	2.55	2.63	2.49	2.68	2.40	2.85	2.31	2.38	1.99
Q-Former+SPLIT2	2.56	2.64	2.50	2.67	2.41	2.83	2.32	2.37	1.99

Instruction Tuning. In our main experiments, we adopt the architecture of InstructBLIP (Dai et al., 2023) for data evaluation and refinement. The learnable projection module is the Q-Former in BLIP2 (Li et al., 2023), the vision encoder is the pre-trained ViT-G/14 from EVA-CLIP (Fang et al., 2023), and the language model is Vicuna-7B (Chiang et al., 2023). Specifically, based on the selected vision encoder and language model, the Q-Former used for instruction tuning has been pre-trained on 129M images (Li et al., 2023), including COCO (Lin et al., 2014), Visual Genome (Krishna et al., 2017), CC3M (Sharma et al., 2018), CC12M (Changpinyo et al., 2021), SBU (Ordonez et al., 2011) and LAION400M (Schuhmann et al., 2021). Based on the official code of InstructBLIP (Dai et al., 2023), the learning hyperparameters during instruction tuning are listed in Table 2. Each dataset has been adopted for tuning on 8 Nvidia A100 (80G) GPUs with the vision encoder and language model kept frozen, only parameters in the Q-Former are optimized.

In addition, we perform data evaluation and refinement using the architecture of LLaVA (Liu et al., 2023), which adopts the linear layer as the projection module for VL alignment. The vision encoder is the pre-trained ViT-L/14 in CLIP (Radford et al., 2021), and the language model is Vicuna-7B (Chiang et al., 2023). The linear layer used for instruction tuning has been pre-trained on 558K image-text pairs from LAION (Schuhmann et al., 2021), CC (Sharma

et al., 2018) and SBU (Ordonez et al., 2011). We adopt the official code of LLaVA (Liu et al., 2023) for instruction tuning with their default learning hyperparameters, which are given in Table 3. Each dataset has been adopted for tuning on 8 Nvidia A100 (80G) GPUs with the vision encoder and language model kept frozen, and only parameters in the linear layer are optimized.

4.2 DQ Evaluation

By setting each dataset as the tuning one D_T , its one-side qualities measured by other datasets $MQ_{T \rightarrow i}^D (i \neq T)$ are visualized in Fig. 4. The areas enclosed by brown and yellow lines are the largest and smallest, indicating that LLaVA-Reasoning and LRV hold the greatest and poorest comprehensive capability. It follows that LLaVA-Reasoning exhibits the highest DQ and LRV shows the lowest DQ among these datasets, as shown in Table 4 computed by Eq. 2. We infer its reason as that LLaVA-Reasoning includes various problems of which the difficulty varies from low to high. As shown in Fig. 5, easy reasoning problems may be similar to description problems, while hard reasoning problems may require logical thoughts. As a result, LLaVA-Reasoning exhibits the greatest comprehensive capability. Besides, the results achieved on SPLIT1 and SPLIT2 demonstrate a high degree of consistency, indicating that the DQ evaluation can provide common and objective data analysis.

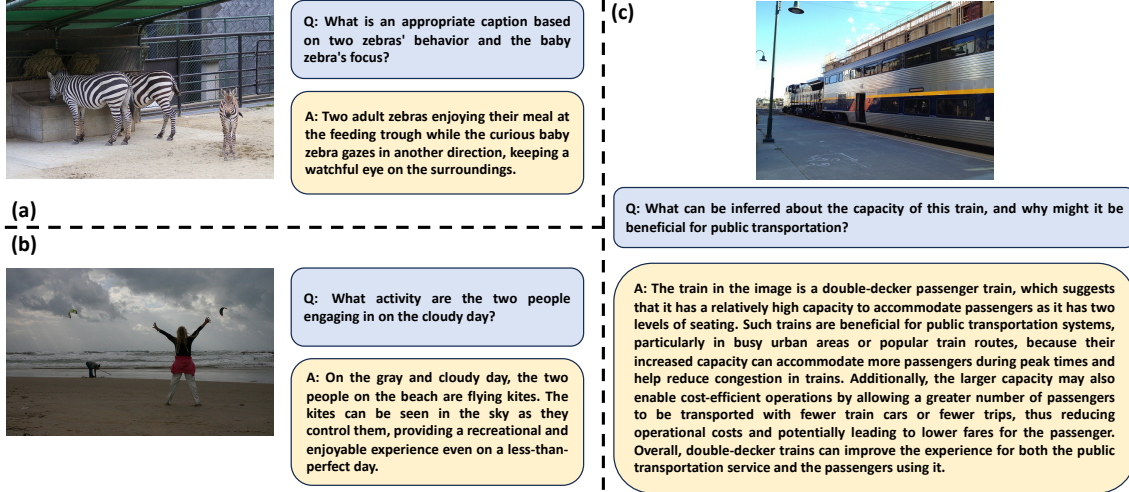


Fig. 5 Three samples in LLaVA-Reasoning. (a) and (b) are easy reasoning problems, and similar to problems of describing images. (c) is a hard reasoning problem requiring logical thoughts. Q: question. A: answer.

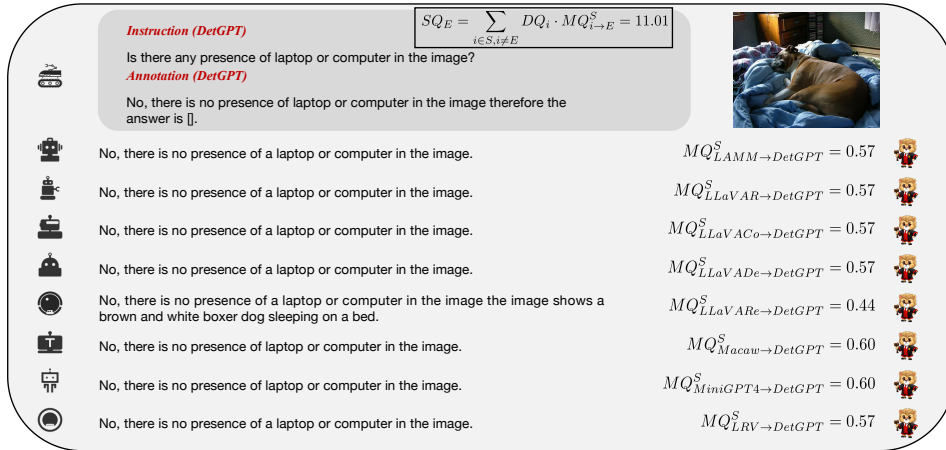


Fig. 6 A sample in DetGPT with high SQ measured by other datasets.

4.3 SQ Evaluation

We show a case of SQ evaluation in Fig. 6. By calculating $MQ_{i \rightarrow E}^S (i \neq E)$ between the generated answers and the annotation, the comprehensive quality of this sample can be obtained. Due to the high similarity among the generated answers, the calculated SQ of this sample is quite high. More evaluation cases of SQ are delivered in Appendix A.

4.4 Ablation Study on MQ and DQ

To validate the rationality of the definition of MQ, based on which DQ is devised, we perform ablation studies on 3 combinations of MQ, in which C1 refers

Eq. 1, C2 and C3 are defined as:

$$\begin{aligned} C2 : MQ &= \text{mean}(B@4 + M + R); \\ C3 : MQ &= \text{mean}(M + R). \end{aligned} \quad (5)$$

Given a dataset, its DQ quantified by a reasonable evaluation criteria should be consistent with its performance in the comprehensive evaluation. By setting *Eval600* as the comprehensive evaluation set and $MQ_{T \rightarrow Eval600}^D$ as the performance quantification, according to the three definitions, the results and relative orders of DQ and $MQ_{T \rightarrow Eval600}^D$ achieved on SPLIT1 are shown in Table 5. Compared with C3, C1 and C2 make more consistent results between DQ evaluation and $MQ_{T \rightarrow Eval600}^D$. Because a dataset

Table 5 Ablation study on the definition of MQ. The blue numbers after the results represent their relative rankings. The bold blue numbers indicate the inconsistent ranking relations.

D_T (Q-Former+SPLIT1)		DetGPT	LAMM	LLaVAR	LLaVACo	LLaVADE	LLaVARE	Macaw	MiniGPT-4	LRV
C1	DQ	2.55 (4)	2.63 (3)	2.49 (5)	2.68 (2)	2.40 (6)	2.85 (1)	2.31 (8)	2.38 (7)	1.99 (9)
	$MQ_{T \rightarrow Eval600}^D$	1.37 (3)	1.35 (4)	1.27 (5)	1.42 (2)	1.16 (6)	1.54 (1)	1.11 (8)	1.13 (7)	0.78 (9)
C2	DQ	2.48 (5)	2.61 (3)	2.57 (4)	2.66 (2)	2.38 (8)	2.73 (1)	2.46 (6)	2.40 (7)	2.20 (9)
	$MQ_{T \rightarrow Eval600}^D$	0.64 (5)	0.70 (3)	0.69 (4)	0.73 (1)	0.57 (8)	0.71 (2)	0.63 (6)	0.59 (7)	0.49 (9)
C3	DQ	2.79 (6)	2.95 (3)	2.94 (4)	3.00 (2)	2.72 (8)	3.05 (1)	2.83 (5)	2.72 (7)	2.59 (9)
	$MQ_{T \rightarrow Eval600}^D$	0.50 (6)	0.56 (3)	0.57 (2)	0.59 (1)	0.47 (8)	0.54 (4)	0.53 (5)	0.48 (7)	0.44 (9)

Table 6 $MQ_{T \rightarrow Eval600}^D$ on SPLIT1 and SPLIT2 by using the Q-Former based architecture.

D_T	DetGPT	LAMM	LLaVAR	LLaVACo	LLaVADE	LLaVARE	Macaw	MiniGPT-4	LRV	Merge
Q-Former+SPLIT1	1.37	1.35	1.27	1.42	1.16	1.54	1.11	1.13	0.78	1.64
Q-Former+SPLIT2	1.38	1.36	1.29	1.43	1.18	1.55	1.12	1.12	0.79	1.64

owning higher DQ should exhibit better all-sided ability, and perform better in the comprehensive evaluation, C1 and C2 are more rational than C3. To preserve a more general evaluation covering as many metrics as possible, we choose C1 as the final definition of MQ, based on which DQ and SQ are devised.

4.5 Single Dataset VS. Merged Dataset

To build a comprehensive dataset integrating all capabilities, a simple yet direct way is to add all these single datasets together into one, denoted as ‘‘Merge’’. By setting *Eval600* as the evaluation dataset, the $MQ_{T \rightarrow Eval600}^D$ achieved by setting each single dataset and the merged dataset as tuning one D_T is compared in Table 6. The simply merged dataset achieves the greatest result, showing adding all datasets together can contribute to an all-powerful model that exhibits the best performance on the comprehensive evaluation set covering all capabilities.

4.6 REVO-LION and Ablation Study on Refinement Strategy

It has been validated that combining all datasets together can develop an all-powerful model in a comprehensive evaluation compared with single datasets in Sec. 4.5. Considering that data quality is more significant than data quantity (Zeng et al., 2023), we further perform data refinement based on the above holistic evaluation. Specifically, we collect part of the samples from each dataset to build a comprehensive dataset. In addition to the refinement strategy defined in Eq. 4, denoted as $S1$, we design another two strategies for comparisons. The second strategy, namely $S2$, collects the samples from each dataset randomly

with the same amount as in $S1$. The third strategy $S3$ adopts the Gaussian distribution for sample selection. Specifically, for each dataset $D_i (i \in S)$, we calculate the mean value μ_i and the standard deviation σ_i of SQ of the samples in D_i . The sample whose SQ exists within an interval of λ times the standard deviation σ_i around the mean value μ_i will be selected. $S3$ is formulated as:

$$S3 = \bigcup_{i \in S} \mathbf{x}_i^k, \quad (6)$$

$$(\mathbf{x}_i^k \in D_i, SQ_i^k \in [\mu_i - \lambda \cdot \sigma_i, \mu_i + \lambda \cdot \sigma_i]).$$

We adopt CIDEr, the hold-out metric in defining MQ, to measure the comprehensive performance of the model tuned on the refined dataset, thus making an objective evaluation for the data refinement. By setting *Eval600* as the comprehensive evaluation set, and selecting a portion P of samples in each dataset, the result comparisons between $S1$ and $S2$ are given in Table 7. The case when $P = 100\%$ refers to simply adding all datasets together.

For the refinement strategy $S1$, the results when $P \in [50\%, 90\%]$ are all competitive and even better than those when using the simply merged dataset. It shows that $S1$ successfully collects high-quality samples in the refined dataset. Specifically, the CIDEr rises with the increase of P from 10% to 70%. When we select the top 50% samples with higher SQ from each dataset, we can already achieve competitive performance comparable to those using the entire data. Then, the CIDEr achieves the highest when $P = 70\%$. When P increases from 70% to 100%, the CIDEr results decrease, which is caused by the involvement of samples with lower SQ. Besides, comparing $S1$

Table 7 Evaluation on *Eval600* measured by CIDEr using refinement strategies *S1* and *S2* with the portion *P* ranging from 10% to 100%. “Nums” refers to the number of image-instruction-answer triplets, that are selected by our scheme from raw datasets, in the refined dataset for tuning. Compared with the results marked with gray achieved by all data, the results marked with yellow achieved with half of the full data are competitive, and the results marked with red are all better.

Portion (<i>P</i>)		10%	20%	30%	40%	50%	60%	70%	80%	90%	100%
Q-Former+SPLIT1	Nums	92828	185650	278473	371293	464115	556940	649760	742584	835406	928225
	S1-CIDEr	163.43	168.56	171.64	174.54	175.13	177.21	194.70	177.16	176.64	175.49
	S2-CIDEr	165.21	168.63	170.18	171.91	172.82	174.37	174.22	175.62	176.03	175.49
Q-Former+SPLIT2	Nums	92807	185608	278410	371211	464012	556815	649616	742418	835219	928017
	S1-CIDEr	165.03	170.87	173.56	174.89	175.99	178.33	178.87	178.23	178.80	175.49
	S2-CIDEr	165.81	169.49	172.40	173.89	175.78	176.23	177.16	178.23	179.17	175.49

Table 8 Evaluation on *Eval600* measured by CIDEr using the refinement strategy *S3* by setting $\lambda \in [1.0, 1.5, 2.0]$. “Nums” refers to the number of image-instruction-answer triplets.

Times (λ)		1.0	1.5	2.0
Q-Former+SPLIT1	Nums	697374	838771	880426
	CIDEr	173.94	175.07	176.52
Q-Former+SPLIT2	Nums	697346	838650	880206
	CIDEr	175.88	178.45	179.32

with *S2*, when keeping the number of collected samples from each dataset the same, results achieved by selecting samples with higher SQ are almost better than those achieved by random selection, which validates that *S1* is more effective than *S2*. Moreover, for the refinement strategy *S2*, the CIDEr rises with the increase of *P* from 10% to 90%. It demonstrates that with the lack of effective data evaluation and refinement strategies, a direct way for improving the performance is just expanding the scale of datasets.

In addition, results from the refinement strategy *S3* when setting the times λ within [1.0, 1.5, 2.0] are given in Table 8. Comparing the results achieved by setting $\lambda = 1.0$ in *S3* with those achieved by setting $P = 70\%$ in *S1* in Table 7, though more samples are collected in *S3*, the performance achieved by *S1* with fewer samples is better. The same phenomenon also happens in the comparison between setting $\lambda \in [1.5, 2.0]$ in *S3* and setting $P = 90\%$ in *S1* in Table 7. The comparisons prove that *S1* is more effective than *S3*. According to the ablation studies, the effectiveness of the proposed *tune-cross-evaluation* paradigm and the refinement strategy is systematically validated.

4.7 Data Evaluation and Refinement using the Linear Projection Module

For a supplementary, we perform the data evaluation and refinement using SPLIT1 based on the architecture adopting the linear layer as the projection module

for VL alignment. Specifically, we take the architecture of LLaVA (Liu et al., 2023), and its setting has been illustrated in Sec 4.1. When setting each dataset as the tuning one D_T , its one-side qualities $MQ_{T \rightarrow i}^D (i \neq T)$ measured by other datasets are given in Fig. 7 (Left). It shows that each dataset exhibits extremely high similarity in the dataset-wise evaluation, leading to almost equal DQ for each dataset, compared with the results in Fig. 4. Consequently, using the linear projection-based VLIT model cannot effectively distinguish differences among datasets, resulting in invalid data evaluation. In addition, based on the evaluation, we perform the data refinement using strategies *S1* and *S2*. The refinement results achieved by using the Q-Former and the linear layer for projection are shown in Fig. 7 (Right). Obviously, when keeping both the vision encoder and the language model frozen, using the linear projection module results in a much more unsatisfying performance than using the Q-Former. Then, taking a deep comparison between the results achieved by *S1* and *S2* using the linear layer-based architecture, the CIDEr results vary within a small range when the portion *P* of selected samples in each dataset changes. The highest result in *S1* refinement, which is higher than using all the data, is achieved when only collecting 10% of samples with higher SQ from each dataset. It shows that as a much simpler projection module, the linear layer does not need as much high-quality instruction data as the Q-Former. The simplicity of the projection module limits the greatest performance that can be improved by expanding the data scale. Besides, compared with *S2*, the strategy *S1* is almost better with different portions.

Except for the effectiveness of *S1*, which has been validated compared with *S2*, other results are inconsistent with ones using the architecture of Instruct-BLIP, and the linear projection module is not as good as the Q-Former. We make the deep analysis as follows. (1) From the perspective of the architecture,

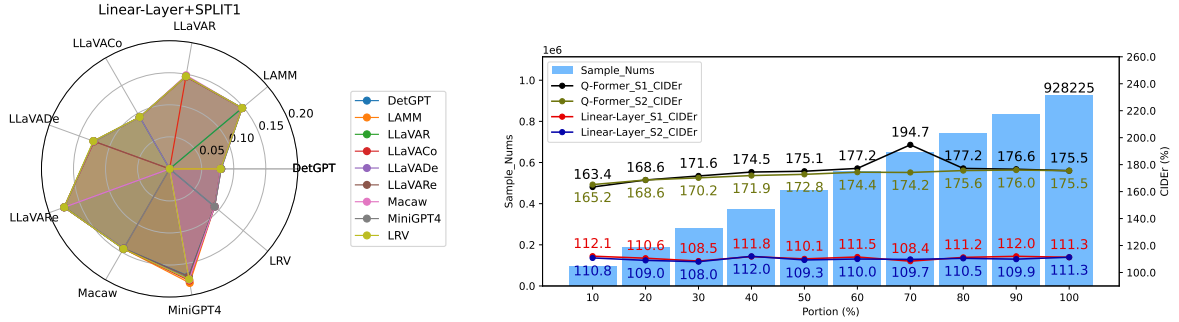


Fig. 7 Results of data evaluation and refinement using the linear projection-based architecture. (Left) Visualizations of $MQ_{T \rightarrow i}^D (i \neq T)$ in DQ evaluation using the linear projection module. (Right) Result comparisons between using the Q-Former and the linear layer for projection using strategies S1 and S2.

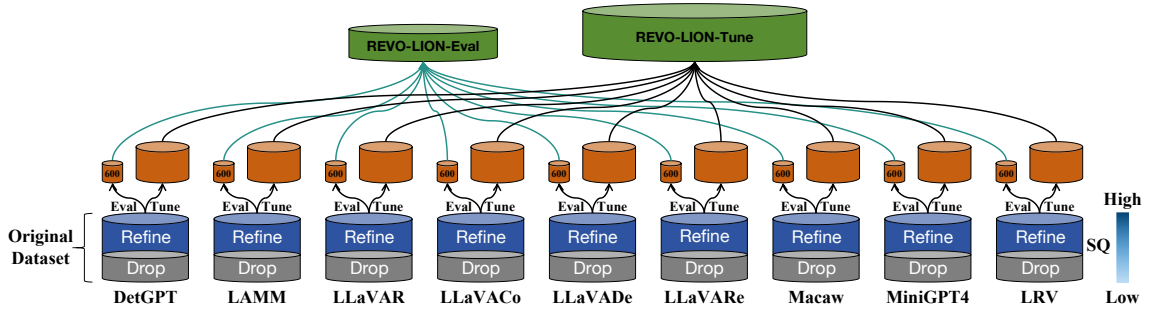


Fig. 8 The refining process of building REVO-LION from existing VLIT datasets. The proposed *tune-cross-evaluation* paradigm is directly performed on each original dataset without partition. After the holistic evaluation, the top 70% samples with higher SQ in each dataset are collected, in which 600 samples are collected into the balanced and comprehensive evaluation benchmark, namely REVO-LION-Eval, and the remaining are collected into the refined tuning dataset, namely REVO-LION-Tune, for developing an all-powerful model.

linear projection is quite simple in transferring the visual feature to the language space. While Q-Former adopts the pre-trained BERT (Kenton and Toutanova, 2019) as initialization, and extracts the desired visual feature according to the texts using a more sophisticated cross-attention mechanism. (2) From the perspective of the pre-trained dataset, both the linear layer and the Q-Former have been pre-trained on large-scale image-text pairs for VL alignment before instruction tuning. As demonstrated in Sec 4.1, Q-Former in BLIP2 (Li et al., 2023) has been pre-trained on 129M images (Li et al., 2023) from COCO (Lin et al., 2014), Visual Genome (Krishna et al., 2017), CC3M (Sharma et al., 2018), CC12M (Changpinyo et al., 2021), SBU (Ordonez et al., 2011) and LAION400M (Schuhmann et al., 2021). While the linear layer in LLaVA (Liu et al., 2023) has been pre-trained only on 558K image-text pairs from LAION (Schuhmann et al., 2021), CC (Sharma et al., 2018) and SBU (Ordonez et al., 2011). The significant difference between the amount of pre-training dataset

results in a much poorer VL alignment of the linear projection than the Q-Former.

5 REVO-LION Release

According to the validated effectiveness on specific data preparation in above experiments, to release the REVO-LION, the evaluation and refinement are performed on the original datasets without partitions. As analyzed in Sec. 4.7, using the linear layer as the projection module for VL alignment is inferior to using the Q-Former. Therefore, we adopt the architecture of InstructBLIP, the detailed setting of which is delivered in Sec 4.1, for data evaluation and refinement.

In the released dataset REVO-LION, the *tune-cross-evaluation* paradigm is directly performed on each original dataset without partition, as shown in Fig 8. According to the results in Table 7, setting the portion $P = 70\%$ can achieve the best performance. Therefore, we release the dataset with setting $P = 70\%$. After refining each dataset, we divide it

into a train set for instruction tuning and an evaluation set as a convenient yet stable benchmark. To keep a balanced dataset for evaluation, we select 600 samples from each refined dataset to build the evaluation set, namely REVO-LION-Eval. The remaining samples in each refined dataset are combined into the instruction tuning dataset, namely REVO-LION-Tune. Moreover, as the annotations in REVO-LION share the same style of open-ended texts generated by LLMs, the caption metrics can be directly adopted for a model-free and human-free performance evaluation when using the REVO-LION-Eval as the benchmark.

6 Conclusions and Outlook

In this paper, we pioneer the analysis of VLIT datasets and propose the *tune-cross-evaluation* paradigm. The key idea is to fully use the datasets as both tuning and evaluation sets, by which the ideal annotations consistent with open-ended generated texts are available. Then, we define the Meta Quality (MQ), a model-free and human-free metric, as the mean score measured by caption metrics, including BLEU, METEOR and ROUGE-L. We extend MQ to Dataset Quality (DQ) and Sample Quality (SQ) for quantitative evaluation. Based on the holistic evaluation, we build a refined dataset REVO-LION by collecting samples with higher SQ from each dataset. With only half of the full data, the model trained on the refined dataset can achieve competitive performance compared to that trained on all data. In the released version, REVO-LION includes a train set, which can be commonly used for developing an all-powerful model, and an evaluation set, which can serve as a convenient yet stable benchmark.

The evaluation paradigm is not limited to the datasets analyzed in this paper. The more datasets with various capabilities are involved in the evaluation, the more comprehensive analysis is achieved. As a result, the refined dataset can be used to develop a VLIT model performing well in more aspects, and also as a more comprehensive evaluation benchmark.

Acknowledgments. This work was partly supported at the university side, by National Science Foundation of China (62222607, 92370201, 62002252), and Shanghai Municipal Science and Technology Major Project (2021SHZDZX0102).

Data Availability. There is no new dataset included in this paper. The datasets in our experiments are all publicly available, they are: DetGPT (Pi et al., 2023),

LAMM (Yin et al., 2023), LLaVAR (Zhang et al., 2023), LLaVA (Liu et al., 2023), Macaw (Lyu et al., 2023), MiniGPT4 (Zhu et al., 2023) and LRV (Liu et al., 2023).

References

- Pi, R., Gao, J., Diao, S., Pan, R., Dong, H., Zhang, J., Yao, L., Han, J., Xu, H., Zhang, L.K.T.: Detgpt: Detect what you need via reasoning. arXiv preprint arXiv:2305.14167 (2023)
- Yin, Z., Wang, J., Cao, J., Shi, Z., Liu, D., Li, M., Sheng, L., Bai, L., Huang, X., Wang, Z., et al.: Lamm: Language-assisted multi-modal instruction-tuning dataset, framework, and benchmark. arXiv preprint arXiv:2306.06687 (2023)
- Zhang, Y., Zhang, R., Gu, J., Zhou, Y., Lipka, N., Yang, D., Sun, T.: Llavav: Enhanced visual instruction tuning for text-rich image understanding. arXiv preprint arXiv:2306.17107 (2023)
- Liu, H., Li, C., Wu, Q., Lee, Y.J.: Visual instruction tuning. arXiv preprint arXiv:2304.08485 (2023)
- Lyu, C., Wu, M., Wang, L., Huang, X., Liu, B., Du, Z., Shi, S., Tu, Z.: Macaw-llm: Multi-modal language modeling with image, audio, video, and text integration. arXiv preprint arXiv:2306.09093 (2023)
- Zhu, D., Chen, J., Shen, X., Li, X., Elhoseiny, M.: Minigpt-4: Enhancing vision-language understanding with advanced large language models. arXiv preprint arXiv:2304.10592 (2023)
- Liu, F., Lin, K., Li, L., Wang, J., Yacoob, Y., Wang, L.: Aligning large multi-modal model with robust instruction tuning. arXiv preprint arXiv:2306.14565 (2023)
- OpenAI: GPT-4 Technical Report (2023)
- Dai, W., Li, J., Li, D., Tiong, A.M.H., Zhao, J., Wang, W., Li, B., Fung, P., Hoi, S.: InstructBLIP: Towards General-purpose Vision-Language Models with Instruction Tuning (2023)
- Luo, G., Zhou, Y., Ren, T., Chen, S., Sun, X., Ji, R.: Cheap and quick: Efficient vision-language instruction tuning for large language models. arXiv

- preprint arXiv:2305.15023 (2023)
- Li, B., Zhang, Y., Chen, L., Wang, J., Yang, J., Liu, Z.: Otter: A multi-modal model with in-context instruction tuning. arXiv preprint arXiv:2305.03726 (2023)
- Chen, D., Liu, J., Dai, W., Wang, B.: Visual instruction tuning with polite flamingo. arXiv preprint arXiv:2307.01003 (2023)
- Chiang, W.-L., Li, Z., Lin, Z., Sheng, Y., Wu, Z., Zhang, H., Zheng, L., Zhuang, S., Zhuang, Y., Gonzalez, J.E., Stoica, I., Xing, E.P.: Vicuna: An Open-Source Chatbot Impressing GPT-4 with 90%* ChatGPT Quality (2023). <https://lmsys.org/blog/2023-03-30-vicuna/>
- Touvron, H., Lavril, T., Izacard, G., Martinet, X., Lachaux, M.-A., Lacroix, T., Rozière, B., Goyal, N., Hambro, E., Azhar, F., et al.: Llama: Open and efficient foundation language models. arXiv preprint arXiv:2302.13971 (2023)
- Xu, P., Shao, W., Zhang, K., Gao, P., Liu, S., Lei, M., Meng, F., Huang, S., Qiao, Y., Luo, P.: Lvlm-ehub: A comprehensive evaluation benchmark for large vision-language models. arXiv preprint arXiv:2306.09265 (2023)
- Liu, Y., Duan, H., Zhang, Y., Li, B., Zhang, S., Zhao, W., Yuan, Y., Wang, J., He, C., Liu, Z., et al.: Mmbench: Is your multi-modal model an all-around player? arXiv preprint arXiv:2307.06281 (2023)
- Yu, W., Yang, Z., Li, L., Wang, J., Lin, K., Liu, Z., Wang, X., Wang, L.: Mm-vet: Evaluating large multimodal models for integrated capabilities. arXiv preprint arXiv:2308.02490 (2023)
- Krizhevsky, A., et al.: Learning multiple layers of features from tiny images (2009)
- Lu, P., Mishra, S., Xia, T., Qiu, L., Chang, K.-W., Zhu, S.-C., Tafjord, O., Clark, P., Kalyan, A.: Learn to explain: Multimodal reasoning via thought chains for science question answering. *Advances in Neural Information Processing Systems* **35**, 2507–2521 (2022)
- Fang, Y., Wang, W., Xie, B., Sun, Q., Wu, L., Wang, X., Huang, T., Wang, X., Cao, Y.: Eva: Exploring the limits of masked visual representation learning at scale. In: *Proceedings of the IEEE/CVF Conference on Computer Vision and Pattern Recognition*, pp. 19358–19369 (2023)
- Ordonez, V., Kulkarni, G., Berg, T.: Im2text: Describing images using 1 million captioned photographs. *Advances in neural information processing systems* **24** (2011)
- Schuhmann, C., Kaczmarczyk, R., Komatsuzaki, A., Katta, A., Vencu, R., Beaumont, R., Jitsev, J., Coombes, T., Mullis, C.: Laion-400m: Open dataset of clip-filtered 400 million image-text pairs. In: *NeurIPS Workshop Datacentric AI* (2021). Jülich Supercomputing Center
- Sharma, P., Ding, N., Goodman, S., Soricut, R.: Conceptual captions: A cleaned, hypernymed, image alt-text dataset for automatic image captioning. In: *Proceedings of the 56th Annual Meeting of the Association for Computational Linguistics (Volume 1: Long Papers)*, pp. 2556–2565 (2018)
- Changpinyo, S., Sharma, P., Ding, N., Soricut, R.: Conceptual 12m: Pushing web-scale image-text pre-training to recognize long-tail visual concepts. In: *Proceedings of the IEEE/CVF Conference on Computer Vision and Pattern Recognition*, pp. 3558–3568 (2021)
- Ouyang, L., Wu, J., Jiang, X., Almeida, D., Wainwright, C., Mishkin, P., Zhang, C., Agarwal, S., Slama, K., Ray, A., et al.: Training language models to follow instructions with human feedback. *Advances in Neural Information Processing Systems* **35**, 27730–27744 (2022)
- Zeng, A., Liu, X., Du, Z., Wang, Z., Lai, H., Ding, M., Yang, Z., Xu, Y., Zheng, W., Xia, X., et al.: Glm-130b: An open bilingual pre-trained model. arXiv preprint arXiv:2210.02414 (2022)
- Du, Z., Qian, Y., Liu, X., Ding, M., Qiu, J., Yang, Z., Tang, J.: Glm: General language model pretraining with autoregressive blank infilling. In: *Proceedings of the 60th Annual Meeting of the Association for Computational Linguistics (Volume 1: Long Papers)*, pp. 320–335 (2022)
- Peng, B., Li, C., He, P., Galley, M., Gao, J.: Instruction tuning with gpt-4. arXiv preprint arXiv:2304.03277

- (2023)
- Ding, N., Chen, Y., Xu, B., Qin, Y., Zheng, Z., Hu, S., Liu, Z., Sun, M., Zhou, B.: Enhancing chat language models by scaling high-quality instructional conversations. arXiv preprint arXiv:2305.14233 (2023)
- Zhou, C., Liu, P., Xu, P., Iyer, S., Sun, J., Mao, Y., Ma, X., Efrat, A., Yu, P., Yu, L., et al.: Lima: Less is more for alignment. arXiv preprint arXiv:2305.11206 (2023)
- Taori, R., Gulrajani, I., Zhang, T., Dubois, Y., Li, X., Guestrin, C., Liang, P., Hashimoto, T.B.: Stanford Alpaca: An Instruction-following LLaMA model. GitHub (2023)
- Wang, Y., Kordi, Y., Mishra, S., Liu, A., Smith, N.A., Khashabi, D., Hajishirzi, H.: Self-instruct: Aligning language model with self generated instructions. arXiv preprint arXiv:2212.10560 (2022)
- Li, J., Li, D., Savarese, S., Hoi, S.: Blip-2: Bootstrapping language-image pre-training with frozen image encoders and large language models. arXiv preprint arXiv:2301.12597 (2023)
- Su, Y., Lan, T., Li, H., Xu, J., Wang, Y., Cai, D.: Pandagpt: One model to instruction-follow them all. arXiv preprint arXiv:2305.16355 (2023)
- Ye, Q., Xu, H., Xu, G., Ye, J., Yan, M., Zhou, Y., Wang, J., Hu, A., Shi, P., Shi, Y., et al.: mplug-owl: Modularization empowers large language models with multimodality. arXiv preprint arXiv:2304.14178 (2023)
- Fu, C., Chen, P., Shen, Y., Qin, Y., Zhang, M., Lin, X., Qiu, Z., Lin, W., Yang, J., Zheng, X., et al.: Mme: A comprehensive evaluation benchmark for multimodal large language models. arXiv preprint arXiv:2306.13394 (2023)
- Zeng, Y., Zhang, H., Zheng, J., Xia, J., Wei, G., Wei, Y., Zhang, Y., Kong, T.: What matters in training a gpt4-style language model with multimodal inputs? arXiv preprint arXiv:2307.02469 (2023)
- Bitton, Y., Bansal, H., Hessel, J., Shao, R., Zhu, W., Awadalla, A., Gardner, J., Taori, R., Schimdt, L.: Visit-bench: A benchmark for vision-language instruction following inspired by real-world use. arXiv preprint arXiv:2308.06595 (2023)
- Aiello, E., Yu, L., Nie, Y., Aghajanyan, A., Oguz, B.: Jointly training large autoregressive multimodal models. arXiv preprint arXiv:2309.15564 (2023)
- Radford, A., Kim, J.W., Hallacy, C., Ramesh, A., Goh, G., Agarwal, S., Sastry, G., Askell, A., Mishkin, P., Clark, J., et al.: Learning transferable visual models from natural language supervision. In: International Conference on Machine Learning, pp. 8748–8763 (2021). PMLR
- Lin, T.-Y., Maire, M., Belongie, S., Hays, J., Perona, P., Ramanan, D., Dollár, P., Zitnick, C.L.: Microsoft coco: Common objects in context. In: Computer Vision–ECCV 2014: 13th European Conference, Zurich, Switzerland, September 6–12, 2014, Proceedings, Part V 13, pp. 740–755 (2014). Springer
- Krishna, R., Zhu, Y., Groth, O., Johnson, J., Hata, K., Kravitz, J., Chen, S., Kalantidis, Y., Li, L.-J., Shamma, D.A., et al.: Visual genome: Connecting language and vision using crowdsourced dense image annotations. International journal of computer vision **123**, 32–73 (2017)
- Kenton, J.D.M.-W.C., Toutanova, L.K.: Bert: Pre-training of deep bidirectional transformers for language understanding. In: Proceedings of NAACL-HLT, pp. 4171–4186 (2019)

A SQ Evaluation Cases

Based on the proposed *tune-cross-evaluation* paradigm, for each dataset, we show several samples with high SQ and low SQ from Fig. 9 to Fig. 25.

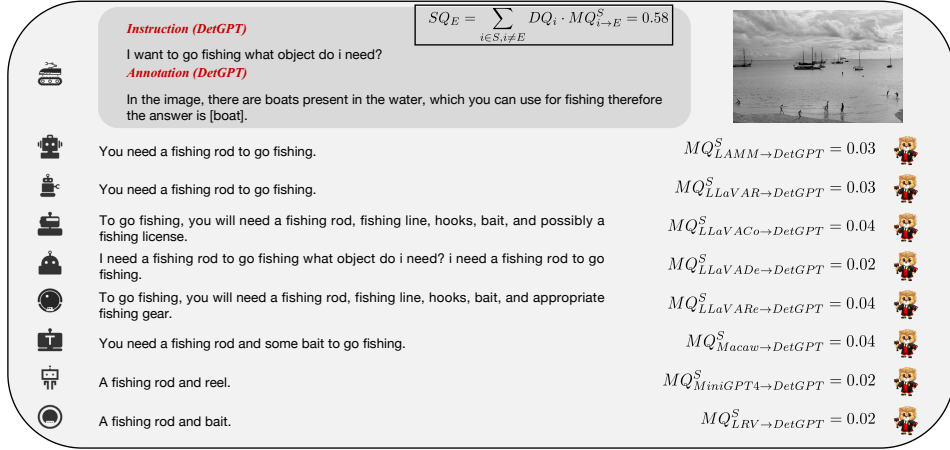


Fig. 9 A sample in DetGPT with low SQ measured by other datasets.

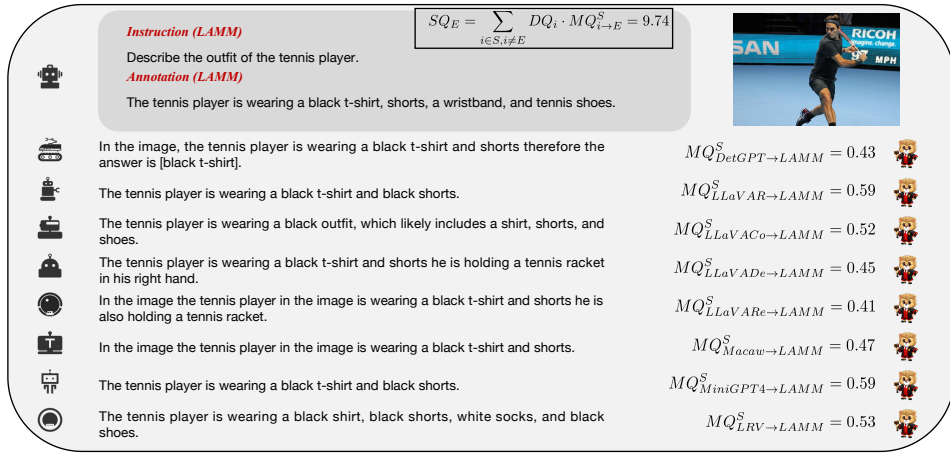


Fig. 10 A sample in Lamm with high SQ measured by other datasets.

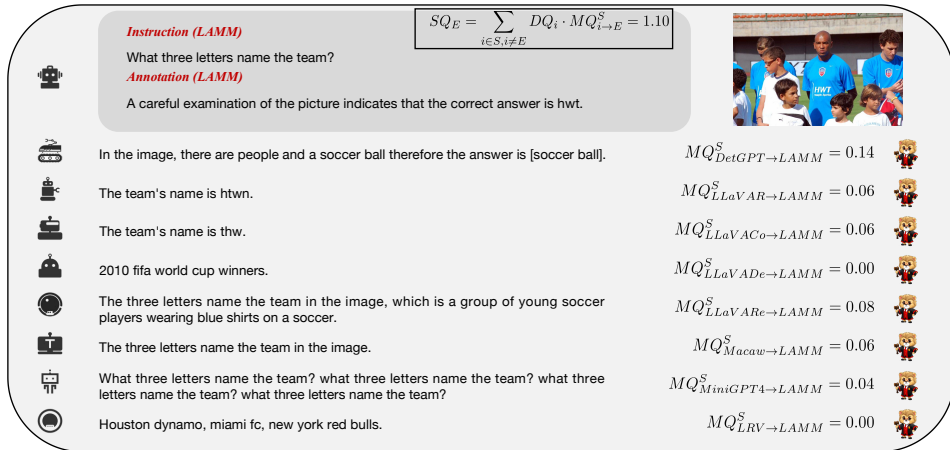


Fig. 11 A sample in Lamm with low SQ measured by other datasets.

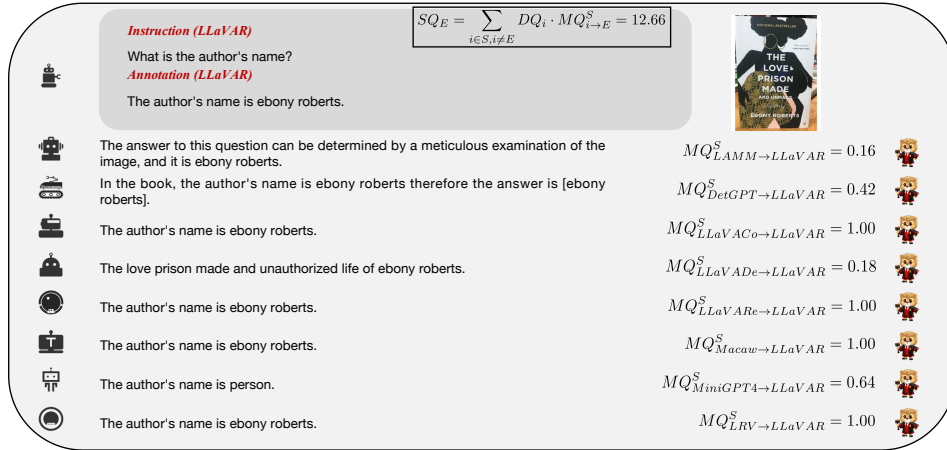


Fig. 12 A sample in LLaVAR with high SQ measured by other datasets.

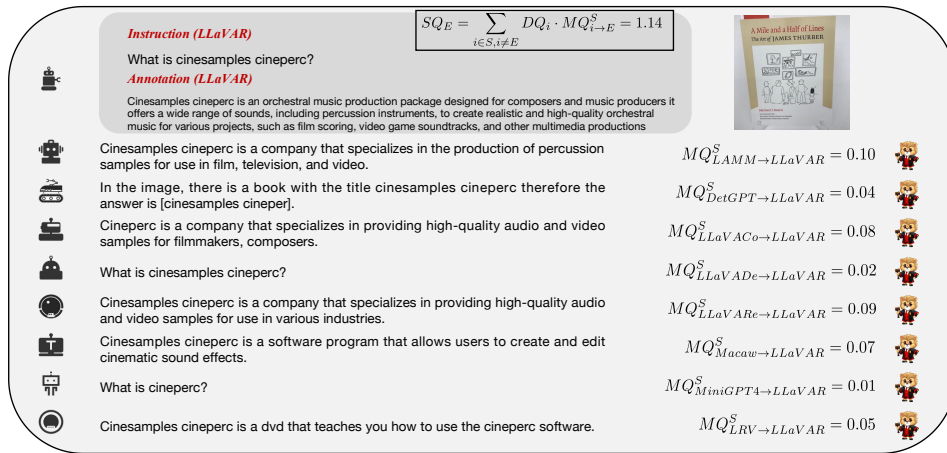


Fig. 13 A sample in LLaVAR with low SQ measured by other datasets.

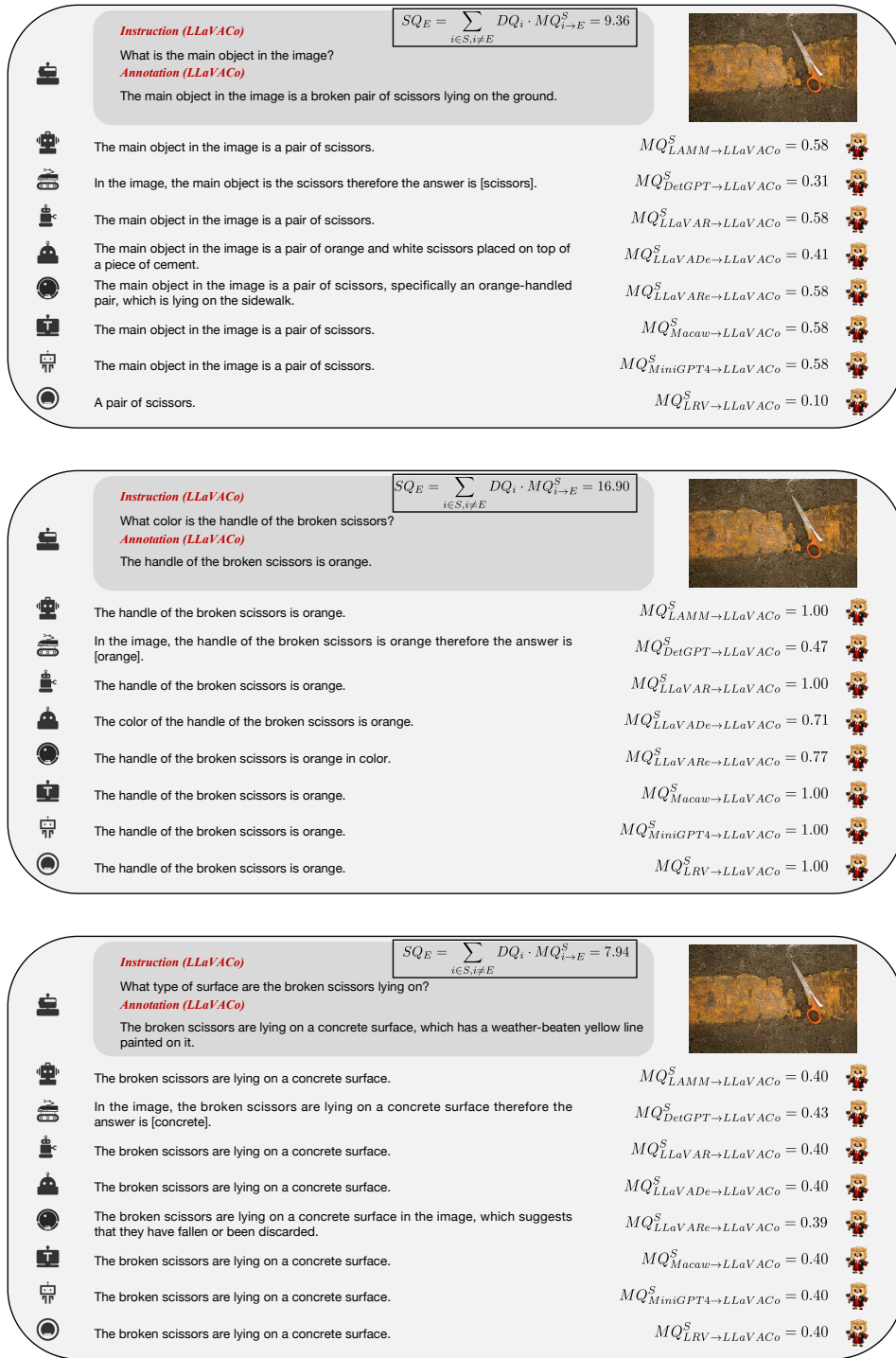


Fig. 14 A conversation sample in LLaVA-Conversation with high SQ measured by other datasets.

Instruction (LLaVACo)

What type of trick is the skateboarder performing?

Annotation (LLaVACo)

Based on the image, a specific trick name cannot be confidently provided however, one can see that the skateboarder is skillfully maneuvering his board in the air, which demonstrates his expertise and talent in the sport.

$$SQ_E = \sum_{i \in S, i \neq E} DQ_i \cdot MQ_{i \rightarrow E}^S = 1.32$$



	The skateboarder is performing a trick where he is riding his skateboard down a ramp.	$MQ_{LAMM \rightarrow LLaVACo}^S = 0.07$	
	In the image, the skateboarder is performing a trick called a kickflip therefore the answer is [kickflip].	$MQ_{DetGPT \rightarrow LLaVACo}^S = 0.12$	
	The skateboarder is performing a trick on a ramp.	$MQ_{LLaVAR \rightarrow LLaVACo}^S = 0.03$	
	The skateboarder is performing a trick on a ramp.	$MQ_{LLaVADe \rightarrow LLaVACo}^S = 0.04$	
	In the image, the skateboarder is performing a trick where he is riding his skateboard on top of a wooden ramp.	$MQ_{LLaVArE \rightarrow LLaVACo}^S = 0.13$	
	The skateboarder is performing a trick on a ramp.	$MQ_{Macaw \rightarrow LLaVACo}^S = 0.05$	
	The skateboarder is performing a trick on a ramp.	$MQ_{MiniGPT4 \rightarrow LLaVACo}^S = 0.04$	
	The skateboarder is performing a trick.	$MQ_{LRV \rightarrow LLaVACo}^S = 0.03$	

Instruction (LLaVACo)

What should skateboarders consider for their safety during skateboarding?

Annotation (LLaVACo)

For their safety, skateboarders should take several precautions while skating, especially when performing tricks or riding in skate parks or urban environments some important safety measures include 1 wearing appropriate protective gear it is essential to wear a well-fitted helmet to protect the head from injuries during falls or collisions.

$$SQ_E = \sum_{i \in S, i \neq E} DQ_i \cdot MQ_{i \rightarrow E}^S = 0.91$$



	Skateboarders should always prioritize safety while skateboarding, they should wear protective gear such as helmets, knees.	$MQ_{LAMM \rightarrow LLaVACo}^S = 0.05$	
	There are skateboarders and person in the image, skateboarders should consider wearing protective gear such as helmets, knees.	$MQ_{DetGPT \rightarrow LLaVACo}^S = 0.05$	
	Skateboarders should always wear protective gear such as helmets, knee pads, elbow pads.	$MQ_{LLaVAR \rightarrow LLaVACo}^S = 0.04$	
	Skateboarding is a popular recreational activity, but it can be dangerous if proper safety measures are not taken into consideration skateboarders.	$MQ_{LLaVADe \rightarrow LLaVACo}^S = 0.04$	
	Skateboarders should consider several factors to ensure their safety during skateboarding first, they should always wear protective gear.	$MQ_{LLaVArE \rightarrow LLaVACo}^S = 0.08$	
	Skateboarders should consider wearing protective gear such as helmets, knee pads, and elbow pads.	$MQ_{Macaw \rightarrow LLaVACo}^S = 0.05$	
	Skateboarding can be a fun and exciting activity, but it can also be dangerous if proper safety precautions are not taken.	$MQ_{MiniGPT4 \rightarrow LLaVACo}^S = 0.02$	
	Skateboarders should wear protective gear such as helmets, knee pads, elbow pads, and wrist.	$MQ_{LRV \rightarrow LLaVACo}^S = 0.04$	

Fig. 15 A conversation sample in LLaVA-Conversation with low SQ measured by other datasets.

Instruction (LLaVADe)

Write a detailed description of the given image.

Annotation (LLaVADe)

In the image, a young boy is sitting on a chair at a dining table with a plate of food in front of him he appears to be cutting a dessert, such as a donut or bagel, using a knife and fork the boy seems to be smiling and looking.

$$SQ_E = \sum_{i \in S, i \neq E} DQ_i \cdot MQ_{i \rightarrow E}^S = 5.91$$



	The image captures a heartwarming scene of a young boy engrossed in his meal he is seated at a wooden table.	$MQ_{LAMM \rightarrow LLaVADe}^S = 0.11$	
	In the image, there is a boy sitting at a dining table with a plate of food in front of him he is using a knife.	$MQ_{DetGPT \rightarrow LLaVADe}^S = 0.34$	
	The image shows a young boy sitting at a table with a plate of food in front of him he appears to be enjoying his meal.	$MQ_{LLaVAR \rightarrow LLaVADe}^S = 0.32$	
	In the image, a young boy is sitting at a wooden table with a plate of food in front of him he is holding a knife.	$MQ_{LLaVACo \rightarrow LLaVADe}^S = 0.37$	
	In the image, a young boy is sitting at a dining table with a plate of food in front of him he is using a fork.	$MQ_{LLaVArE \rightarrow LLaVADe}^S = 0.41$	
	The image shows a young boy sitting at a table with a plate of food in front of him.	$MQ_{Macaw \rightarrow LLaVADe}^S = 0.22$	
	This image shows a young boy sitting at a table with a plate of food in front of him he is using a knife and fork to cut.	$MQ_{MiniGPT4 \rightarrow LLaVADe}^S = 0.36$	
	A young boy wearing glasses is sitting at a wooden table with a green plate in front of him, holding a spoon and fork.	$MQ_{LRV \rightarrow LLaVADe}^S = 0.22$	

Fig. 16 A sample in LLaVA-Detailed description with high SQ measured by other datasets.

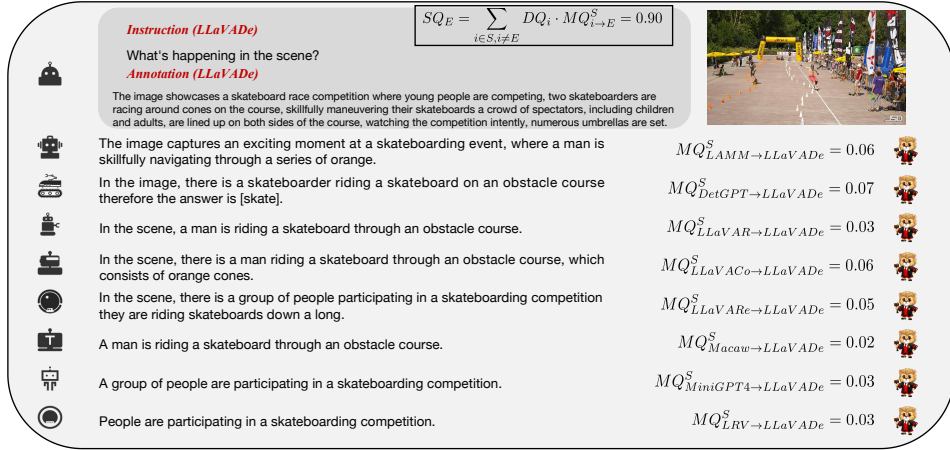


Fig. 17 A sample in LLaVA-Detailed description with low SQ measured by other datasets.

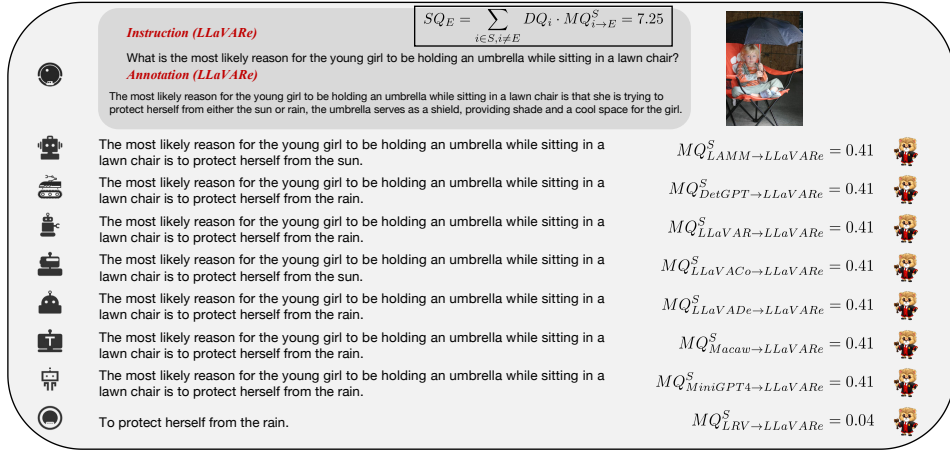


Fig. 18 A sample in LLaVA-Reasoning with high SQ measured by other datasets.

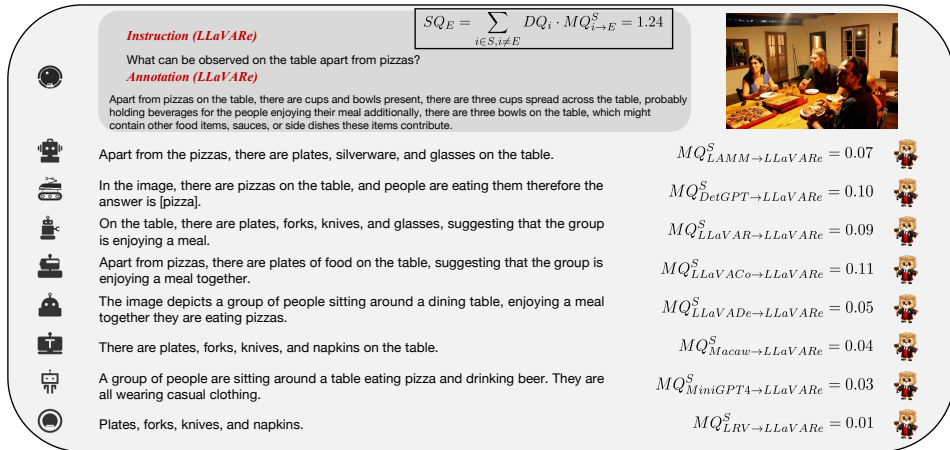


Fig. 19 A sample in LLaVA-Reasoning with low SQ measured by other datasets.

Instruction (Macaw)

What is the name of the technique used to fold paper in the creation of the collared shirt and tie in the image?

Annotation (Macaw)

The technique used to fold paper in the creation of the collared shirt and tie in the image is likely origami.

$$SQ_E = \sum_{i \in S, i \neq E} DQ_i \cdot MQ_{i \rightarrow E}^S = 13.03$$



-  The technique used to fold paper in the creation of the collared shirt and tie is called origami.
-  The technique used to fold paper in the creation of the collared shirt and tie is called origami therefore the answer is [origami].
-  The technique used to fold paper in the creation of the collared shirt and tie is called origami.
-  The technique used to fold paper in the creation of the collared shirt and tie is called origami.
-  The technique used to fold paper in the creation of the collared shirt and tie is called origami this traditional japanese art.
-  The name of the technique used to fold paper in the creation of the collared shirt and tie in the image is origami.
-  The technique is called origami.

$MQ_{L\text{AMM} \rightarrow \text{Macaw}}^S = 0.72$ 

$MQ_{\text{DetGPT} \rightarrow \text{Macaw}}^S = 0.65$ 

$MQ_{L\text{LaV}\text{AR} \rightarrow \text{Macaw}}^S = 0.72$ 

$MQ_{L\text{LaV}\text{ACo} \rightarrow \text{Macaw}}^S = 0.72$ 

$MQ_{L\text{LaV}\text{ADe} \rightarrow \text{Macaw}}^S = 0.72$ 

$MQ_{L\text{LaV}\text{ARe} \rightarrow \text{Macaw}}^S = 0.69$ 

$MQ_{\text{MiniGPT4} \rightarrow \text{Macaw}}^S = 0.81$ 

$MQ_{L\text{RV} \rightarrow \text{Macaw}}^S = 0.07$ 

Fig. 20 A sample in Macaw with high SQ measured by other datasets.

Instruction (Macaw)

What kinds of dangers might be involved in performing this kind of activity?

Annotation (Macaw)

Some dangers might include falling, getting injured, or hitting objects in the surrounding environment.

$$SQ_E = \sum_{i \in S, i \neq E} DQ_i \cdot MQ_{i \rightarrow E}^S = 1.18$$



-  While skateboarding can be a fun and exciting activity, there are several dangers involved in performing tricks like the one depicted.
-  There are skateboard, person, and backpack in the image performing tricks on a skateboard can be dangerous.
-  There are several dangers involved in performing skateboarding tricks, such as the risk of falling, colliding with obstacles.
-  Performing tricks on a skateboard, such as jumping over a rail or ramp, can pose several dangers to the skate.
-  The image depicts a skateboarder performing a trick on a ramp, jumping high into the air with his skateboard.
-  Performing tricks on a skateboard, such as the one depicted in the image, can involve several dangers firstly.
-  The skateboarder is performing a trick on a ramp in a skate park. He is wearing a white t-shirt.
-  The skateboarder could fall off the skateboard and get injured.

$MQ_{L\text{AMM} \rightarrow \text{Macaw}}^S = 0.07$ 

$MQ_{\text{DetGPT} \rightarrow \text{Macaw}}^S = 0.06$ 

$MQ_{L\text{LaV}\text{AR} \rightarrow \text{Macaw}}^S = 0.08$ 

$MQ_{L\text{LaV}\text{ACo} \rightarrow \text{Macaw}}^S = 0.06$ 

$MQ_{L\text{LaV}\text{ADe} \rightarrow \text{Macaw}}^S = 0.02$ 

$MQ_{L\text{LaV}\text{ARe} \rightarrow \text{Macaw}}^S = 0.08$ 

$MQ_{\text{MiniGPT4} \rightarrow \text{Macaw}}^S = 0.03$ 

$MQ_{L\text{RV} \rightarrow \text{Macaw}}^S = 0.05$ 

Fig. 21 A sample in Macaw with low SQ measured by other datasets.

Instruction (MiniGPT4)

Could you describe the contents of this image for me?

Annotation (MiniGPT4)

This image shows a helicopter flying over the ocean with a large ship in the background the helicopter appears to be a military.

$$SQ_E = \sum_{i \in S, i \neq E} DQ_i \cdot MQ_{i \rightarrow E}^S = 8.83$$



-  This image showcases a large military helicopter, the sikorsky uh-60 black hawk, in mid-air.
-  In the image, there is a helicopter flying over the ocean with a boat in the background therefore, the image contains a helicopter.
-  The image depicts a helicopter flying over the ocean with a ship in the background.
-  The image depicts a military helicopter, specifically a us navy seahawk helicopter, flying over the ocean.
-  The image depicts a large military helicopter flying over the ocean, with a ship in the background the helicopter appears to be.
-  The image depicts a large military helicopter flying over the ocean, with a ship in the background the helicopter appears to be.
-  The image depicts a military helicopter flying over the ocean.
-  A helicopter flying over the ocean with a ship in the background.

$MQ_{L\text{AMM} \rightarrow \text{MiniGPT4}}^S = 0.15$ 

$MQ_{\text{DetGPT} \rightarrow \text{MiniGPT4}}^S = 0.49$ 

$MQ_{L\text{LaV}\text{AR} \rightarrow \text{MiniGPT4}}^S = 0.48$ 

$MQ_{L\text{LaV}\text{ACo} \rightarrow \text{MiniGPT4}}^S = 0.33$ 

$MQ_{L\text{LaV}\text{ADe} \rightarrow \text{MiniGPT4}}^S = 0.72$ 

$MQ_{L\text{LaV}\text{ARe} \rightarrow \text{MiniGPT4}}^S = 0.72$ 

$MQ_{\text{Macaw} \rightarrow \text{MiniGPT4}}^S = 0.23$ 

$MQ_{L\text{RV} \rightarrow \text{MiniGPT4}}^S = 0.41$ 

Fig. 22 A sample in MiniGPT-4 with high SQ measured by other datasets.

Instruction (MiniGPT4)

Please provide a detailed description of the picture.

Annotation (MiniGPT4)

The image shows a row of clocks with different times on them. The clock on the left reads 12:00, the one in the middle reads 3:00, and the one on the right reads 6:00. The clocks have white faces and black hands. They are arranged in a straight line, slightly overlapping each other. They are mounted on a white wall, and there is nothing else in the image.

$$SQ_E = \sum_{i \in S, i \neq E} DQ_i \cdot MQ_{i \rightarrow E}^S = 1.86$$


The first image depicts a tidy home office desk setting in the center of the desk, there is a laptop placed.

In the image there are six clocks arranged in a line on a white background, with each clock showing a different time in different cities.

The picture shows a white wall with five clocks on it, each representing different cities around the world.

The picture features four clocks arranged in a row on a white background the clocks are lined up side by side and show different time zones.

The image depicts a white wall with five clocks displayed on it, each representing a different time zone the clocks are arranged.

The image depicts a white wall with four clocks displayed on it, each representing a different time zone the clocks are lined up.

The image depicts a group of clocks arranged in a line on a white background.

There is a white wall with four clocks on it, each showing the time in different cities new york, london, tokyo.

$MQ_{Lamm \rightarrow MiniGPT4}^S = 0.07$

$MQ_{DetGPT \rightarrow MiniGPT4}^S = 0.12$

$MQ_{LLaVAR \rightarrow MiniGPT4}^S = 0.06$

$MQ_{LLaVACo \rightarrow MiniGPT4}^S = 0.12$

$MQ_{LLaVADe \rightarrow MiniGPT4}^S = 0.14$

$MQ_{LLaVARE \rightarrow MiniGPT4}^S = 0.09$

$MQ_{Macaw \rightarrow MiniGPT4}^S = 0.08$

$MQ_{LRV \rightarrow MiniGPT4}^S = 0.05$

Fig. 23 A sample in MiniGPT-4 with low SQ measured by other datasets.

Instruction (LRV)

How many bears appear in the water and how many are on rocks?

Annotation (LRV)

There are two bears on rocks and one bear in the water.

$$SQ_E = \sum_{i \in S, i \neq E} DQ_i \cdot MQ_{i \rightarrow E}^S = 11.56$$


There are two bears in the water and one bear on rocks.

In the image, there are two bears visible, one on the rocks and the other in the water therefore the answer is [2].

There are two bears in the water and one bear on rocks.

There are two bears in the water and two bears on rocks.

There are two bears in the water and two bears on rocks.

There are two bears in the water and one bear on rocks in the image the two bears in the water are swimming or wading.

There are two bears in the water and two bears on rocks.

There are two bears in the water and two bears on rocks.

$MQ_{Lamm \rightarrow LRV}^S = 0.67$

$MQ_{DetGPT \rightarrow LRV}^S = 0.35$

$MQ_{LLaVAR \rightarrow LRV}^S = 0.67$

$MQ_{LLaVACo \rightarrow LRV}^S = 0.62$

$MQ_{LLaVADe \rightarrow LRV}^S = 0.62$

$MQ_{LLaVARE \rightarrow LRV}^S = 0.40$

$MQ_{Macaw \rightarrow LRV}^S = 0.62$

$MQ_{MiniGPT4 \rightarrow LRV}^S = 0.62$

Instruction (LRV)

Are there any animals in this image?

Annotation (LRV)

No, there are no animals in the image.

$$SQ_E = \sum_{i \in S, i \neq E} DQ_i \cdot MQ_{i \rightarrow E}^S = 11.64$$


No, there are no animals visible in this image.

In the image, there are no animals present therefore the answer is [].

No, there are no animals in this image.

No, there are no animals in this image.

No, there are no animals in this image the scene depicts a large group of people gathered in a grassy field, flying kites.

No, there are no animals in this image it appears to be a group of people gathered in a grassy field, engaging in various activities.

No, there are no animals in this image.

No, there are no animals in this image.

$MQ_{Lamm \rightarrow LRV}^S = 0.62$

$MQ_{DetGPT \rightarrow LRV}^S = 0.41$

$MQ_{LLaVAR \rightarrow LRV}^S = 0.75$

$MQ_{LLaVACo \rightarrow LRV}^S = 0.75$

$MQ_{LLaVADe \rightarrow LRV}^S = 0.32$

$MQ_{LLaVARE \rightarrow LRV}^S = 0.29$

$MQ_{Macaw \rightarrow LRV}^S = 0.75$

$MQ_{MiniGPT4 \rightarrow LRV}^S = 0.75$

Fig. 24 Two samples in LRV with high SQ measured by other datasets.

Instruction (LRV)
Rate the image quality from 1 to 10 in terms of clarity and details

Annotation (LRV)
7.

$$SQ_E = \sum_{i \in S, i \neq E} DQ_i \cdot MQ_{i \rightarrow E}^S = 0.00$$



	1 is the poorest quality and 10 is the best quality.	$MQ_{LAMM \rightarrow LRV}^S = 0.00$ 
	The image quality in terms of clarity and details is high therefore the answer is [10].	$MQ_{DetGPT \rightarrow LRV}^S = 0.00$ 
	The image quality is 10, meaning it is very clear and detailed.	$MQ_{LLaVAR \rightarrow LRV}^S = 0.00$ 
	The image quality is a 10, as it provides a clear and detailed view of the young man catching the baseball.	$MQ_{LLaVACo \rightarrow LRV}^S = 0.00$ 
	The image depicts a young man in an orange shirt catching a baseball with a glove he is standing on a grassy field.	$MQ_{LLaVADe \rightarrow LRV}^S = 0.00$ 
	The image quality is rated 8 out of 10 in terms of clarity and details the image shows a young man.	$MQ_{LLaVARE \rightarrow LRV}^S = 0.00$ 
	The image quality is around 8 or 9 in terms of clarity and details.	$MQ_{Macaw \rightarrow LRV}^S = 0.00$ 
	The man is wearing an orange t-shirt and a baseball cap, and he is reaching out to catch the ball with his glove.	$MQ_{MiniGPT4 \rightarrow LRV}^S = 0.00$ 

Fig. 25 A sample in LRV with low SQ measured by other datasets.